IL NUOVO CIMENTO Vol. 28 C, N. 6 Novembre-Dicembre 2005
DOI 10.1393/ncc/i2005-10032-6

Comparison between HF radar current data and moored ADCP currentmeter

S. Cosoli([1]), M. Gačić([2]) and A. Mazzoldi([1])

([1]) *CNR-ISMAR, Istituto di Scienze Marine, Sezione di Ricerca di Venezia - Venice, Italy*
([2]) *Istituto Nazionale di Oceanografia e di Geofisica Sperimentale (OGS) - Trieste, Italy*

(ricevuto il 31 Maggio 2005; revisionato il 14 Novembre 2005; approvato il 20 Novembre 2005; pubblicato online il 18 Gennaio 2006)

Summary. — A preliminary assessment of accuracy of a two-sites shore-based HF Radar network along the Venice Lagoon littoral was attempted by means of comparison with a 57.5 day-long ADCP current time series for the period September-October 2002. Results showed that radar measurements were accurate (< 7 cm/s) in more than 50% of the times, since more than 50% of the differences between both E-W (U) and N-S (V) components were under 7 cm/s, and more than 50% of direction differences were under 35°. The main differences between the HF radar and surface ADCP currents can be explained in terms of random errors affecting the measurement technique and the daily sea breeze forcing, since low-pass filtering of current time series significantly improved the correlation and decreased the RMS of the differences between the two measured data set. Comparison of the semidiurnal (M2, S2) tidal band suggested good agreement between tidal ellipse amplitudes. Wind forcing on a daily time-scale (sea-breeze) was associated with larger differences between radar and ADCP currents at a diurnal band due to the presence of a vertical shear in the surface layer.

PACS 92.60.Gn – Winds and their effects.
PACS 92.10.Sx – Coastal and estuarine oceanography.
PACS 95.75.Wx – Time series analysis, time variability.

1. – Introduction

Surface currents play a fundamental role in a coastal environment because of their influence on ecology, shipping and recreation. The study of surface circulation and its impact on environmental properties requires the acquisition of high-quality current data but, due to instrumental limitation of conventional measurement techniques, direct measurement of surface currents on a wider area with spatial resolution on the order of kilometers is very expensive if not impossible. The improvement of Doppler Radar techniques allowed for remote measurements of the surface currents on larger area, with spatial resolution on the order of kilometers and temporal resolution of one hour. Many radar surface current measurements have been carried out in tide-dominated regions

(semi-enclosed basins, estuaries or channels), where vertical shear is relatively weak and thus, surface and sub-surface current tidal parameters (amplitude and phase) differ to a small extent [1-5]. In most of the comparisons between radar current estimates and those obtained by more conventional techniques, differences of 4–20 cm/s and 60°–70° in speed and direction, respectively, were found [6-8].

Differences between HF radar and currentmeter measurements arise potentially from both instrumental sources and measurement techniques themselves. HF surface measurements represent in fact an integral (both in time and space) of the current data within the first half-a-meter of the water column typically on a 1 km^2 footprint [9], whereas currentmeters measure point-wise the values of the current speed and direction typically at distances larger than 1 m from the sea surface. Thus, the obtained current speed and direction differ in the two measuring devices even if radar and currentmeter are properly operating and perfectly measuring. An assessment of HF radar capabilities on a statistical basis can be attempted by means of comparisons with conventional currentmeters, in order to evaluate intrinsic instrumental limitations and contributions of the so-called "geophysical noise", *i.e.* well-defined physical processes known or supposed to occur such as the vertical and horizontal shear. The comparison between HF radar and the classical current measurements is generally carried out at two levels; the first level consists in comparing the radial currents from an individual radar site and the currentmeter data, while the second level represents a comparison of the current vectors reconstructed from two or more antennas and the moored currentmeter data. In the present paper, the HF radar current vector data were compared with the moored ADCP current measurements over a 57.5 day overlapping period, from September to October 2002, in front of the Venice Lagoon.

The wind record from the area was also analyzed and differences between the two measured data sets were discussed taking into consideration the wind-induced vertical shear. The aim was to provide an upper bound on the accuracy of radar current estimates. All the analyses were carried out using hourly mean data.

The work is organized as follows. In sect. **2**, a brief description of radar systems, ADCP currentmeter setting, current speed and direction time series, as well as analysis methods, were given. Results of statistical analyses of differences between the radar-derived and ADCP currents are shown and discussed in sect. **3**, while sect. **4** gives summary and conclusions.

2. – Measurements and data analysis techniques

2˙1. *HF radar installations.* – A network of shore-based 25 MHz High-Frequency (HF) radar systems (Codar Ocean Sensors (COS), Ltd) was deployed since November 2001 at the islands of Lido and Pellestrina with the aim of long-term monitoring of surface currents in front of the Venice Lagoon (fig. 1). A more detailed description of radar characteristics, data analysis and measurement results for the complete data set can be found in [10].

Each radar site consists of one transmitting and one receiving antenna, and measures radial currents to distances up to 15 km offshore. The basic physical mechanism on which the technology of the HF radars relies is Bragg scattering of electromagnetic waves from surface gravity waves [11], which produces two sharp peaks in the Doppler spectrum. In the absence of surface currents, the two peaks are symmetrical, so that any displacement from their theoretical frequency is related to an underlying current on the basis of deep-water dispersion relation.

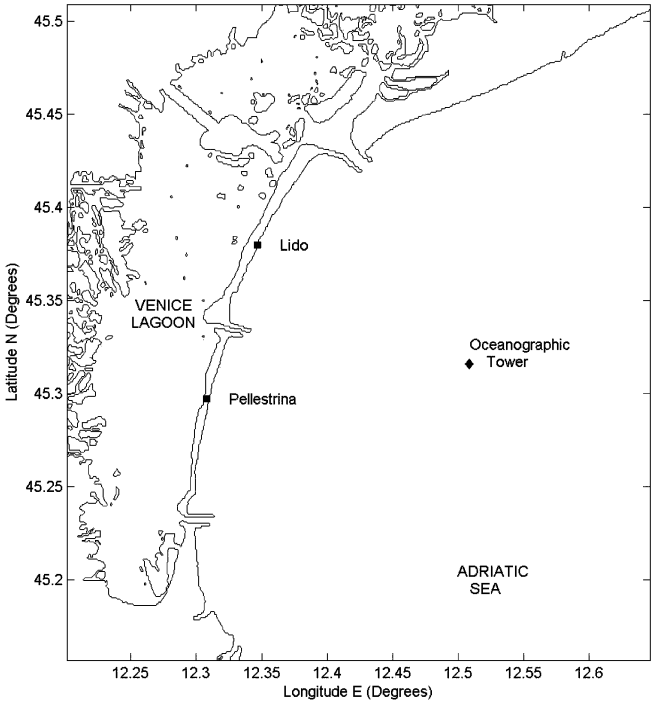

Fig. 1. – Study area. Positions of radar sites are shown by squares, while the ADCP mooring coinciding with the Oceanographic Tower "Acqua Alta" location is denoted by the black diamond.

Complex cross spectra of the received echo for each station were obtained via system software every 2.5 minutes. Every 10 minutes these data were averaged over a time interval of 15 minutes, and then converted into 10-minute radials. These were used for determining the hourly radial velocities at five degrees angular resolution, providing bearing, range and speed. Radial data from the two stations were finally combined to produce hourly maps of current vectors within a regular grid. The vector computations utilized radials within a 30–150 degree sector with respect to the baseline connecting the two antenna locations. Out of that sector, radial velocity uncertainties increased due to increased propagation loss and signal refraction effects [12]. Typical nominal accuracy of total vectors was less than 7 cm/s in magnitude, and less than 10 degrees in direction, as specified by the producer (COS, `http://www.codaros.com/seasonde_specs.htm`).

2˙2. *Moored Acoustic Doppler Current Profiler (ADCP) measurements and wind observations.* – SACLANT Undersea Research Center maintained a bottom-mounted ADCP mooring at the Oceanographic Tower "Acqua Alta" position (12°30.50′ E, 45°18.88′ N) in the period September-December 2002 (see fig. 1). The depth of the mooring was 17 m. A 1200 kHz ADCP was deployed in an upward looking configuration, with 35 cm bin length and 40 cm blanking, and was programmed to measure currents in 35 cm bins using burst sampling with ping every 2 minutes for 16 minutes. The burst was repeated every hour. Velocity data with estimated errors greater than 5 cm/s were excluded; velocity data where more than 60% of the ping had bad data in two or more beams were also ex-

cluded. Bins near the sea surface were excluded because of potential contamination from the surface echo. A magnetic variation correction of 1.53° East of North was applied to data (*Jeffrey Book, personal communication*). The top bin current data that were compared to radar measurements, were recorded at a nominal depth of 2.37 m below the surface. Another possibility would be to extrapolate ADCP data to the free surface and reconstruct the surface current time-series at a constant depth (*Richard Signell, personal communication*). In this paper, however, in order to avoid errors introduced by extrapolations, we decided to neglect the tidal sea level variations and thus consider the data from the bin having a constant distance from the bottom.

Wind data for the analyzed period were obtained by an anemometer located at 15 m above the mean sea level at the Oceanographic Tower. The wind data were then adjusted to the 10 m height above the sea level using a logarithmic law. Hourly time-series of wind speed and direction were then obtained from five-minute data by means of vector-averaging technique.

Hourly time series of wind stress components were obtained following [13], as $\tau_{\langle x,y\rangle} = \rho c_d \langle u, v\rangle |u|$, where ρ is the air density, c_d the wind-speed–dependent drag coefficient, $|u|$ wind speed. $\tau_{\langle x,y\rangle}$ represent eastward and northward components of wind stress in N/m^2.

2˙3. *Tidal analysis*. – In order to extract tidal currents, radar and ADCP current time-series at all depths were analyzed with the aid of the software named *t_tide* [14], written in MATLAB language on the basis of a FORTRAN code [15]. Tidal ellipse parameters (major and minor axes, inclination and phase angle), together with their uncertainties, were obtained for each tidal constituent included in the analysis by the least-square harmonic analysis technique of experimental time-series. Non-tidal currents were then obtained by subtracting the tidal signal from the observed time series. The contribution of tidal currents to the overall variability is expressed as a percentage of the total variance explained by tidal oscillations.

2˙4. *Complex (vector) correlation analysis*. – Time series of wind stress and current vectors can be described in a more compact way by means of complex numbers as $w = u + iv$, where u, v represent the horizontal vector components and i is the imaginary unit. In order to compare two or more vector time series, a complex (vector) correlation coefficient between pairs of vectors is defined as the normalized inner product of the two vectors [16]:

$$R = \rho \exp[i\alpha] = \frac{\langle w_1 \circ w_2 \rangle}{\langle w_1 \circ w_1 \rangle^{1/2} \langle w_2 \circ w_2 \rangle^{1/2}} .$$

The magnitude ρ provides a measure of the "traditional" covariance of vector components over time, representing then a measure of the overall correlation between the two vectors. Assuming a linear dependence between the two time series, the magnitude squared ρ^2 represents the portion of variance of the second time series, which is explained by the first one. The phase angle α represents the average difference in direction (veering) between the two vectors over the same time interval.

If a time lag between the two time series is also considered, the complex correlation coefficient gives rise to a complex lagged correlation function, which reduces to the complex autocorrelation function whenever the two time series are identical. If the two time-series on the contrary are different, a complex cross-correlation function is obtained, allowing for an estimate of the phase-lag between the two series, namely the delay between wind forcing and currents.

TABLE I. – *Basic statistical moments for Codar and ADCP E-W (U) and N-S (V) velocity components for September-October 2002.*

	Codar		ADCP (2.37 m)	
	U (cm/s)	V (cm/s)	U (cm/s)	V (cm/s)
Max	35.6	29.4	39.3	17.7
Min	−32.4	−42.9	−37.6	−43
Mean	−2.1	−5.5	−6.3	−6.5
Std. deviation	10.8	10.7	10.7	8.9
Median	−3.4	−5.7	−7	−6.2
Root-mean-square (RMS)	11	12	12.4	11

3. – Results and discussion

HF radar measurements started on November 2001, and ended in October 2002, while ADCP recording started in September 2002 and ended in December 2002. As a consequence, the comparison between the time-series recorded by the two instruments was carried out for the maximum overlapping period of 57.5 days starting on September 4th, 2002, up to October 31st, 2002. The comparison between radar and ADCP measured currents involved only one radar bin in the whole Codar grid, which coincided with the mooring location. Based on statistics calculated on the first differenced data, hourly current components were checked for spikes, or anomalous values that appeared occasionally due to errors in target speed and bearing determination. Data that did not pass the quality control were marked and subsequently considered as "bad data".

The percentage of "good" radar current estimates was 92.5% of the total record length, giving a result of 102 hours of "bad" radar measurements. Gaps larger than 8 hours rarely occurred in the time series, and the longest one (49 hours) started on October 26th at 7:00. The percentage of "good" data in the ADCP time series reached 87% of the total length in the uppermost bin, corresponding to 177 hours of "bad" current estimates, and an average percentage of 95% along the water column. For the shallowest ADCP bin (2.37 m below the surface), gaps larger than 4 consecutive hours seldom occurred, and the largest gap, 12 hours, occurred from October 15th, 7:00 to 18:00. For spectral calculations, the gaps up to 12 hours in the time-series were filled using linear interpolation. Statistical moments were computed only for the common good data points of both time-series.

Table I summarizes some basic statistics for radar and ADCP current time-series for the shallowest bin, while fig. 2 shows histograms for Codar and for ADCP E-W (U), N-S (V) components. Good agreement was found between radar-derived and ADCP zonal (U) current components for speed range (maxima and minima), standard deviations and root-mean-squares (RMS). The mean appeared to be significantly different, ADCP average of the U component being at least twice as the radar one. Median values, being a more robust estimate of the center of the data sets, showed negative values, and were consistent with the mean southward flow as obtained in [10]. Good agreement for every statistical moment was found for the meridional (V) component, with exception of the maximum

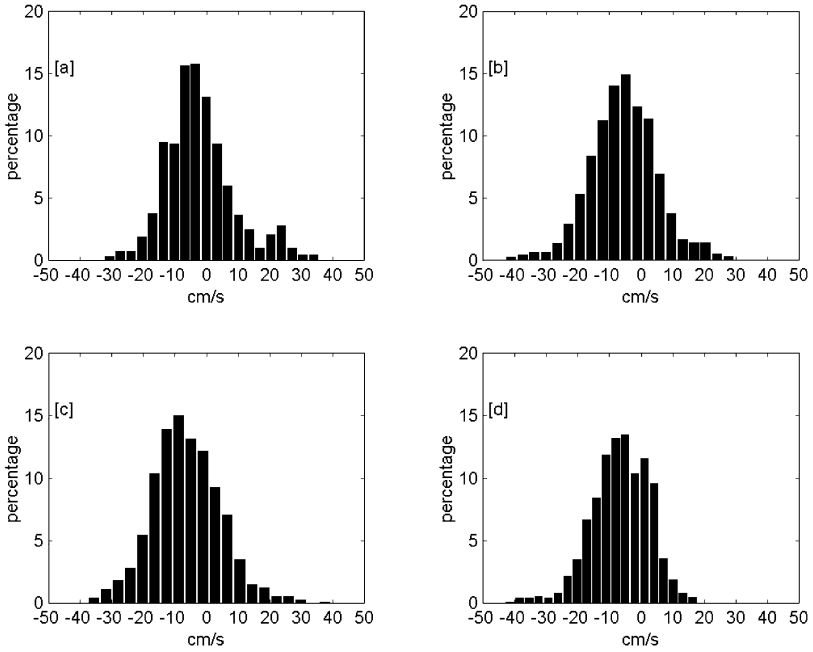

Fig. 2. – Histograms for Codar (a and b) and ADCP (c and d) U (left) and V (right) velocity components.

value that showed radar-derived currents being 12 cm/s greater than the ADCP ones. Statistical tests performed on the mean and the variance of the velocity components, based on the hypothesis of Gaussian distribution, suggested that average values were significantly different for both U and V radar and ADCP current components. On the other hand, current variance was significantly larger in Codar than ADCP V component, while no statistically significant differences existed in U component variance.

Dispersion diagrams between pairs of velocity components measured by radar and ADCP gave a qualitative view of the reliability of the measurements: if the two time series represent the same quantity, the scatter plot was expected to be a straight line. According to the dispersion diagrams of the two horizontal components obtained by radar and ADCP for the shallowest bin, depicted in fig. 3, the velocity estimates were quite nicely clustered along the line of equal velocity. Computing the scalar correlation coefficient at zero lag gave 0.65 for the U component, and 0.48 for the V component; the RMS of the differences between estimates is 9.31 cm/s, and 9.64 cm/s for the U and V component, respectively, while the RMS of direction differences was 85°. Similar plots and quantities can be obtained for each ADCP bin along the water column with respect to radar measurements. In general, moving from surface towards the bottom, the correlation between radar and ADCP measurements decreased while the RMS increases both for the velocity components and for direction as well. For example, the ADCP bin located 6 meter below the sea surface showed still good agreement with the surface measurements, the RMS of the differences and the correlation coefficients being respectively 9.88 cm/s and 0.51 for the U component, 10.69 cm/s and 0.32 for the V component. The RMS difference for the flow direction was 97°. Anyway, over the entire water column RMS

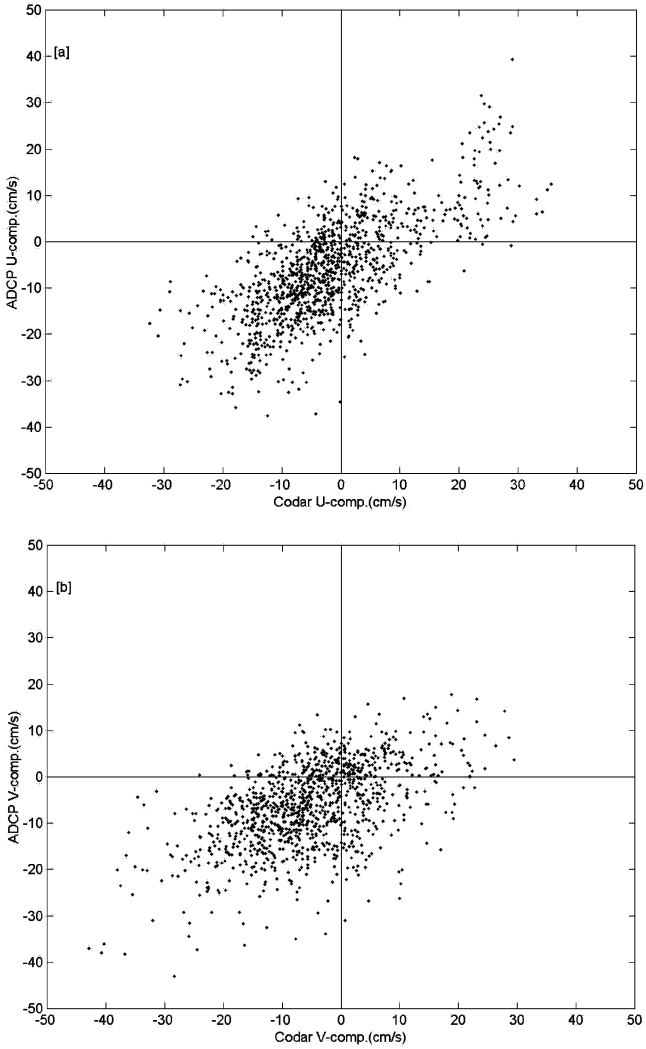

Fig. 3. – Dispersion diagrams of the U (a) and V (b) Codar and ADCP current components.

did not exceed 12 cm/s for both U and V components, while for direction RMS did not exceed 120°. Table II summarizes the statistics for U and V component differences between radar and ADCP current time series, which were depicted in the two histograms in fig. 4. The range of velocity differences had the same order of magnitude as the U and V velocity components for both radar and ADCP currents. The shape of the two histograms was Gaussian-like, and shifted towards positive values for the U component while more symmetrically clustered around zero mean for the V component, as suggested by both the mean and the median values.

In order to compare the direction of the flow estimated by the two instruments, the angles between the Codar and ADCP current vectors for different depths were calculated; their frequency distribution functions were presented in fig. 5. Positive angle means that

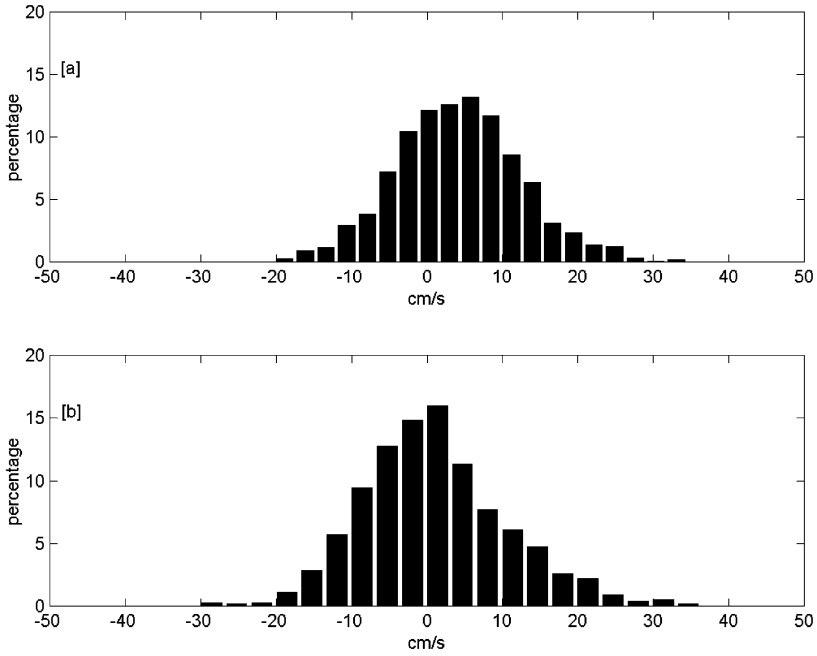

Fig. 4. – Histograms of the differences between ADCP and Codar measured U (a) and V (b) current components.

the ADCP current vector was to the right of the Codar currents and vice versa, negative values of the angle stayed for the ADCP currents being to the left of the Codar vectors. Frequency distribution function of the angle between the ADCP currents of the surface cell and the Codar current vectors was rather symmetric around the most frequent angle and close to the normal distribution. Moving to deeper layers, the function became more flat and for the deepest cell it showed a bi-modal structure with a secondary frequency maximum close to the angle of 180° between the surface (Codar) and ADCP currents

TABLE II. – *Basic statistical moments for Codar and ADCP E-W (U) and N-S (V) velocity component differences for September-October 2002.*

	U-component differences (cm/s)	V-component differences (cm/s)
Max	34.4	36.3
Min	−20.2	−30.2
Mean	4.2	0.9
Std. deviation	8.4	9.6
Median	4.1	0.23
Root-mean-square (RMS)	9.3	9.6

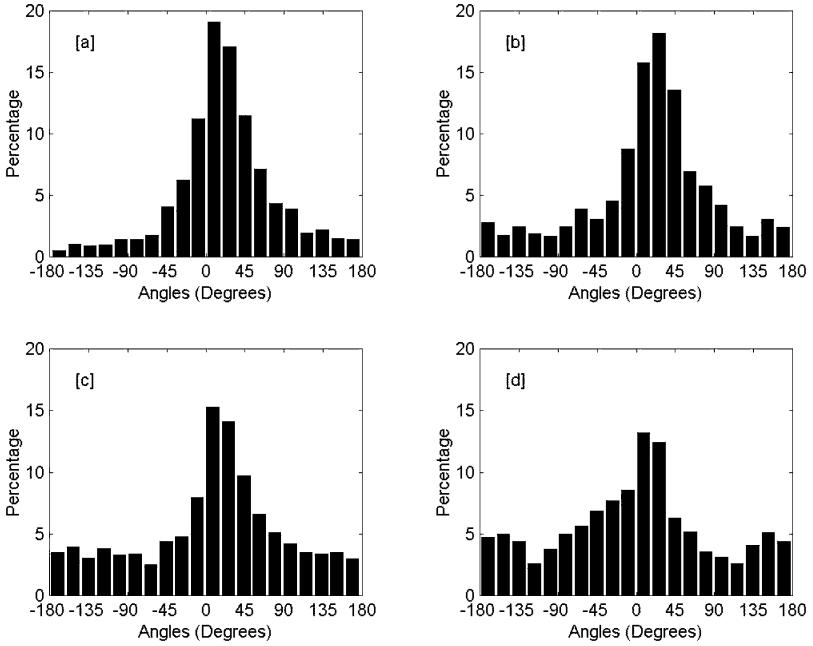

Fig. 5. – Frequency distribution of angles between Codar and ADCP measured currents at four different depths: a) 2.37 m; b) 5.87 m; c) 9.37 m; d) 16.37 m.

recorded at that cell, *i.e.* 16 m below the mean sea level. The most frequent value of the angle between the surface ADCP cell and the Codar current vector was about 20° with the median value of 19° meaning a clockwise vertical shear consistent with the Ekman dynamics. Root-mean-square was 62°.

Complex correlation between radar and ADCP current at zero lag was 0.63, and a 15° veering angle was found between radar-derived and subsurface ADCP currents. U component differences at zero lag were weakly correlated with E-W wind stress component (0.11, respectively), and correlation increased slightly between V component differences and N-S wind stress components (0.23).

Statistics improved if current speed and direction were low-passed with a 4th-order Butterworth filter [17]: high-frequency "tidal noise" was removed; correlation increased, and RMS differences between surface and subsurface current estimates were significantly reduced. Scalar correlation coefficients and RMS of the differences between radar and ADCP currents at zero lag were 0.72, 0.58, 6.9 cm/s and 6.0 cm/s for the U and V component, respectively, and 67° for current direction. Complex (vector) correlation coefficient slightly improved correlation between current time series, while the average veering of the two time series decreased to 12°. After low-passing current time series, U component differences were uncorrelated with wind stress E-W component, correlation being only 0.04. On the other side, the differences between current V component were correlated with wind stress (0.25) N-S component. Vector correlation magnitude was almost the same, and the veering was −36°.

Spectral analysis is a useful tool for describing the main properties of radar and currentmeter time series. Rotary spectra, in particular, identify typical spectral bands

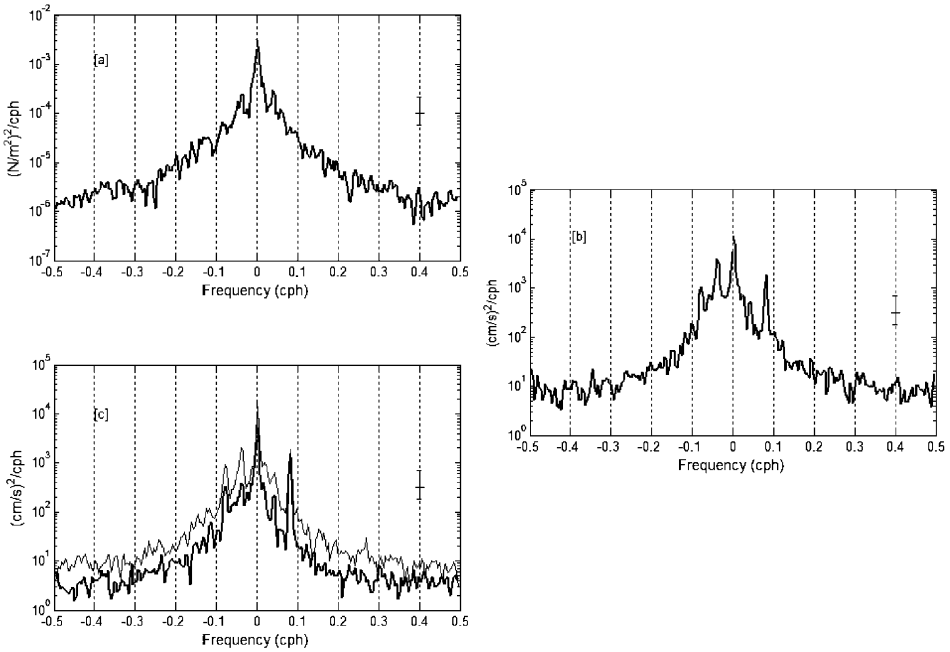

Fig. 6. – Rotary spectrum of wind stress (a), Codar surface currents (b) and ADCP currents (c) at subsurface (continuous line) and bottom (bold line). Vertical error bars denote the 95% confidence level. Negative frequencies refer to the clockwise (anti-cyclonic) motions, while positive frequencies refer to the counterclockwise (cyclonic) motions.

in current and wind fluctuations since they combine spectral information in the U, V components into clockwise and counter-clockwise rotating fluctuations [18]. In order to improve the statistical significance of spectral estimates, rotary spectra were obtained on 256 hours sub-samples (about 10 days) of the interpolated time series.

Rotary spectra for radar currents, ADCP currents and wind velocity were shown in fig. 6. Spectral characteristics were similar for radar and ADCP time series. Low-frequency motions in the radar and ADCP had the same order of magnitude, and no significant high-frequency motions with periods smaller than 10–12 hours were present. Significant peaks existed in current measurements around semidiurnal and diurnal periods. Larger current variance occurred in the clockwise spectrum ("negative" frequencies) in the frequency band spanning from 12 to 26 hours. Radar currents showed peak on the inertial frequency (17 hours), but it was barely resolved with the window length used for spectral calculations, and the low energy level at this frequency, if compared to semidiurnal and diurnal peaks, was probably due to intermittent characteristics of inertial oscillations. The diurnal peak was slightly larger in radar-derived currents than ADCP sub-surface currents, and significantly reduced its amplitude towards the bottom. The amplitude reduction with depth, which involved the whole frequency band from 12 to 26 hours, was probably associated with strong diurnal wind forcing affecting surface and sub-surface currents more than near-bottom currents. A significant diurnal peak was in fact present in wind stress rotary spectrum, although wind variance was more symmetrically distributed around zero-frequency than current variance. A more

TABLE III. – *Tidal ellipse parameters, together with their errors, obtained by least-squares harmonic analysis of radar-derived currents (a), shallowest ADCP bin (b) and wind stress time series (c). Ellipse amplitudes and errors are expressed in cm/s and N/m^2 for currents and wind-stress, respectively. Ellipse inclinations are expressed in degrees counter-clockwise from East, and phase angle in degrees relative to Greenwich time zone.*

(a)

Tide	Frequency (cph)	Maj (cm/s)	Emaj (cm/s)	Min (cm/s)	Emin (cm/s)	Inc (°E)	Einc (°E)	Pha	Epha
Msf	0.0028219	8.1	3.6	1.9	3.4	29	29	272	27
K1	0.0417807	4.6	1.7	−2.7	1.5	27	35	185	38
M2	0.0805114	4.2	1.2	1.5	1.2	150	26	177	21
S2	0.0833333	3.4	1.2	0.4	1.5	145	21	176	19

(b)

Tide	Frequency (cph)	Maj (cm/s)	Emaj (cm/s)	Min (cm/s)	Emin (cm/s)	Inc (°E)	Einc (°E)	Pha	Epha
Msf	0.0028219	8	3.3	−1.3	3.4	30	30	254	27
K1	0.0417807	3.3	1.4	−0.5	1.2	5	19	192	28
M2	0.0805114	4.3	0.9	1.3	1	121	16	161	17
S2	0.0833333	3.2	0.9	1	0.95	120	22	163	22

(c)

Tide	Frequency (cph)	Maj (10×) (N/m^2)	Emaj (10×) (N/m^2)	Min (10×) (N/m^2)	Emin (10×) (N/m^2)	Inc (°E)	Einc (°E)	Pha	Epha
Msf	0.0028219	4.1	2.6	−0.2	2.3	41	41	266	40
K1	0.0417807	1.6	0.6	−0.1	0.8	60	27	190	24
M2	0.0805114	0.3	0.3	0.1	0.3	5	114	23	117
S2	0.0833333	0.4	0.4	−0.06	0.4	148	71	225	80

prominent peak on semidiurnal frequencies in current spectrum occurred in the counter-clockwise spectrum ("positive" frequencies), but no variations in amplitude with depth were noted. This behavior might be explained in terms of tidal oscillations which are prevalently barotropic and thus depth independent.

Harmonic analyses performed on the current time series for each ADCP bin, for radar-derived surface currents, and wind-stress time-series as well, confirmed these results. Table III synthesizes the results for the most energetic tides, namely the long-period (Msf), the diurnal (K1) and semidiurnal (M2, S2) tidal constituents. Astronomical tides accounted for 38% of the total variance for the Codar-derived surface currents, and for 37% of the total variance for the uppermost ADCP bin, showing that tidal forcing was not the most important one for surface and sub-surface current variability. Kinetic

TABLE IV. – *Mean kinetic energy per unit mass for radar-derived currents (a) and its distribution over depth for ADCP current time series. Three depths are considered: (b) subsurface* 2.37 *m; (c) mid-depth* 9.37 *m; (d) bottom* 16.37 *m. Mean kinetic energy is separated into tidal, non-tidal and long-period non-tidal portions. Units are* $(cm/s)^2$.

(a)

Kinetic energy $(cm/s)^2$	Mean	Tidal	Non-tidal	Long-period non-tidal
U component	57	27	30	16
V component	73	15	58	38
Total	130	42	88	54

(b)

Kinetic energy $(cm/s)^2$	Mean	Tidal	Non-tidal	Long-period non-tidal
U component	73	23	50	36
V component	62	12	50	33
Total	135	35	100	69

(c)

Kinetic energy $(cm/s)^2$	Mean	Tidal	Non-tidal	Long-period non-tidal
U component	37	11	26	21
V component	39	18	21	16
Total	76	29	47	37

(d)

Kinetic energy $(cm/s)^2$	Mean	Tidal	Non-tidal	Long-period non-tidal
U component	17	4	13	9
V component	28	11	17	12
Total	45	15	30	21

energy calculations for September-October 2002 current field (table IV), suggested that up to 70% of the fluctuational non-tidal kinetic energy was accounted for by long-period forcing, while the remaining percentage was associated with short time-scale features, such as seiches, inertial motions, or turbulence. Small-scale eddies and coastal jets, in fact, were very prominent in the surface current field outside the Lagoon of Venice, as shown in [10], and in [19].

Harmonic analysis of ADCP and radar-derived currents suggested that a strong ver-

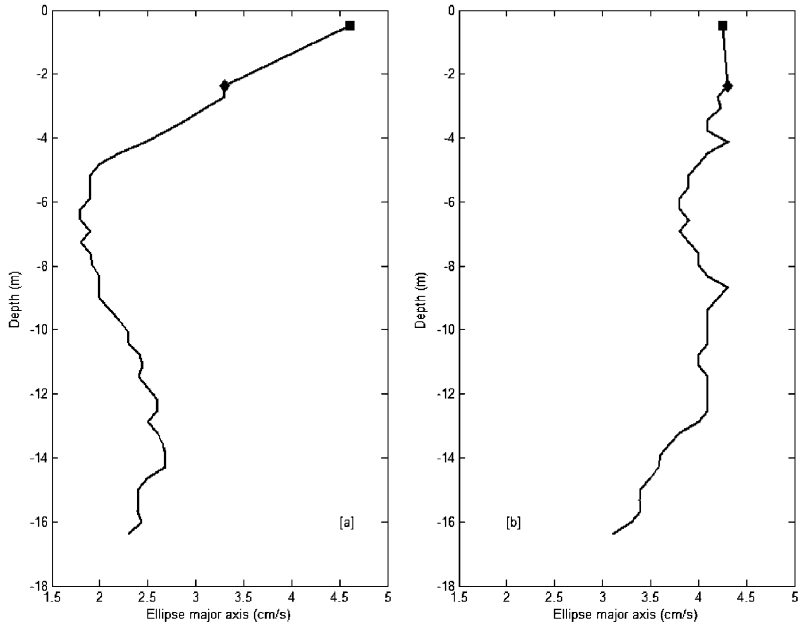

Fig. 7. – Vertical distribution of the major ellipse axis for the K1 (a) and M2 (b) tidal constituents. The first point near the surface is the major axis magnitude obtained from Codar data.

tical shear exists for diurnal tidal constituent (K1), which was probably due to the fact that part of the variance at that frequency was generated by wind forcing (fig. 7). This then resulted in a strong discrepancy between the Codar surface currents and recordings at the surface ADCP cell. On the other hand, M2 amplitude varied with depth very weakly and therefore differences between Codar and ADCP were much smaller at the semidiurnal frequency. Importance of the diurnal wind forcing was also evidenced from the occurrence of the statistically significant peak at the 24-hour scale in the wind-stress spectrum. On the other hand, no prominent peak at semidiurnal scale was observed.

4. – Conclusions

In this work, an assessment of 25 MHz Codar-type HF radar network capabilities was attempted by means of the comparison with subsurface current estimates obtained by a bottom-mounted ADCP. The comparison was done over a two-months period in September-October 2002 for a single-grid point in the Codar domain corresponding to the ADCP location. Basic statistical moments (mean, median, standard deviation, root-mean-square) were calculated for both the velocity components and flow direction, as well as for their differences between Codar and ADCP measurements.

Hourly time-series of surface and subsurface currents were significantly correlated at zero lag, both for scalar and complex correlation; a mean veering of 15 degrees was found between the two current time series. This means that subsurface ADCP current estimates were on the right of the surface Codar-derived currents. The median values of the N-S (V) and E-W (U) component differences were small, and close to zero especially

for the V component. The RMS differences for both velocity components were higher than 7 cm/s, which is the stated accuracy of HF radar technique. According to the sample cumulative distribution for the U, V component and direction differences, more than 43% of the differences between the U component estimates were under 5 cm/s (44% for the V component), more than 55% of the U component differences (56% for the V component) were under 7 cm/s, and more than 50% of direction differences were under 35°. After low-pass filtering of the data, both scalar and vector correlations between velocity components estimates significantly improved. U, V component differences were under 7 cm/s in more than 65% and 75% of the estimates, while direction differences were under 67° in 77% of the estimates. Moreover, almost all direction differences larger than 45° were associated with currents significantly lower than 7 cm/s.

The results of the comparison between radar and ADCP suggested quite a good agreement between the two current data sets, since most of the differences in U, V components and direction were smaller than the RMS values. Assuming ADCP estimates to be error-free, so that all differences were due to radar limitation, radar measurements were accurate (< 7 cm/s) 55% of the times. Similar percentages suggested that average statistics could be strongly affected by a relatively small amount of observations with very large disagreement between estimates. Since low-pass filtering improved significantly correlation coefficients decreasing also the RMS differences, large differences can be thought as arising from random errors and, as shown from harmonic analysis, from wind influence on a diurnal time-scale.

Tidal constituents obtained from subsurface and Codar measurements were also compared, but due to the small signal-to-noise ratios and limited time series length, questions arised on the sensitivity and on the meaning of the tidal analyses results. However, for each tidal constituent included in least-squares harmonic analysis, the major axes of tidal ellipses were larger than the error. On the other hand, the minor ellipse axes and inclination angles estimates were smaller than the error. Following estimates of expected errors on amplitude and phase [20], only semidiurnal tides in current time-series can be considered accurately resolved, so that current variance only in this frequency band was effectively tidally-driven. For these tidal constituents, good agreement was found for ellipse amplitudes, but differences up to 30° were found for ellipse inclinations, which was anyhow within the error limits.

Time series length and noise levels were inadequate to resolve accurately other tidal constituents. There existed some hints that energy in the diurnal band was associated to wind-driven currents, since U and V component differences were correlated with wind stress components. In addition, at the diurnal frequency the vertical shear was very pronounced, suggesting the importance of wind forcing. The sheared wind-driven current was presumably responsible to a large extent for the discrepancy between ADCP and Codar current measurements.

* * *

This research was supported by CORILA (Consortium for Coordination of Research Activities concerning the Venice Lagoon System, between the University of Venice, the University of Padua, the Architectural Institute of Venice, the National Research Council of Italy and the National Institute of Oceanography and Experimental Geophysics—OGS), Venice. We are thankful to J. Book of NRL and R. Signell of the SACLANT Research Center in La Spezia for making available the ADCP data. We are also grateful to R. Signell for his helpful comments on the manuscript.

REFERENCES

[1] Shay L. K., Graber H. C., Ross D. B. and Chapman R. D., *J. Atm. Ocean. Technol.*, **12** (1995) 881.
[2] Hammond T. M., Pattiaratchi C., Eccles D., Osborne M., Nash L. and Collins M., *Cont. Shelf Res.*, **7** (1987) 411.
[3] Prandle D., *J. Phys. Oceanogr.*, **17** (1987) 231.
[4] Prandle D., *Prog. Oceanogr.*, **27** (1991) 403.
[5] Osborne M. J., *J. Soc. Underwater Technol.*, **17** (1991) 10.
[6] Paduan J. D. and Rosenfeld L. K., *J. Geophys. Res.*, **101,** C9 (1996) 20.669.
[7] Graber H. C. and Haus B. K., *J. Geophys. Res.*, **102,** C8 (1997) 18.749.
[8] Chapman R. D., Shay L. K., Graber H. C., Edson J. B., Karachintsev A., Trump C. L. and Ross D. B., *J. Geophys. Res.*, **102,** C8 (1997) 18.737.
[9] Essen H. H., Mittelstaed E. and Schirmer F., *Dtsch. Hydrogr. Z.*, **34** (1981) 1.
[10] Kovačević V., Gačić M., Mancero Mosquera I., Mazzoldi A. and Marinetti S., *J. Mar. Syst.*, **51** (2004) 95.
[11] Crombie D. D., *Nature*, **175** (1955) 681.
[12] Lipa B. J. and Barrick D. E., *IEEE J. Ocean. Eng.*, **OE-8** (1983) 226.
[13] Large W. G. and Pond S., *J. Phys. Oceanogr.*, **11** (1981) 324.
[14] Pawlowicz R., Beardsley B. and Lentz S., *Comp. Geosci.*, **28** (2002) 929.
[15] Foreman M. G. G., 1978. *Manual for Tidal currents analysis and prediction*, Pacific Marine Science Report 78-6, Institute of Ocean Sciences, Patricia Bay, Sidney, British Columbia, Revised edition 1996.
[16] Kundu P. K., *J. Phys. Oceanogr.*, **6** (1976) 238.
[17] Roberts J. and Roberts T. D., *J. Geophys. Res.*, **83** (1978) 5510.
[18] Gonella J., *Deep Sea Res.*, **19** (1972) 833.
[19] Paduan J. D., Gačić M., Kovačević V., Mancero Mosquera I. and Mazzoldi A., Vorticity Patterns Offshore of the Venetian Lagoon from HF Radar Observations. Linea 3.5 *Quantità e Qualità degli Scambi tra Laguna e mare*, WBS1 *Misure dei Parametri Fisici*, WBS1.2. *Misure di Corrente con Radar HF*, Quinto Rapporto di Ricerca, OGS, Relazione RELI-34/2003 OGA-24, 2004.
[20] Godin G., *The Analysis of Tides* (Liverpool University Press) 1972, p. 264.